

Introduction

Tinnitus occurs when damage to the peripheral auditory system leads to spontaneous brain activity that is interpreted as sound. Many types of brain activity show abnormalities in association with tinnitus, but it is not clear which of these relate to the phantom sound itself, as opposed to predisposing factors or secondary consequences. Direct demonstration of the core tinnitus correlates requires high-precision recordings of neural activity combined with a behavioral paradigm in which the perception of tinnitus is manipulated and accurately reported upon by the subject. This has thus far not been possible in animal or human research. Here we present extensive intracranial recordings from an awake, behaving tinnitus patient during short-term modifications in perceived tinnitus loudness, permitting a robust characterization of the core tinnitus brain network.

Methods

A 50 year-old male patient with moderate-to-severe bilateral hearing loss (Fig. 1) and longstanding bilateral tinnitus underwent diagnostic electrocorticographic epilepsy monitoring. He had tinnitus unrelated to his seizure phenomenology. Coverage included high-impedance depth electrodes in left primary auditory cortex and grid electrodes over large parts of left auditory cortex (164 total intracranial electrodes).

To investigate dynamic tinnitus correlates the subject's tinnitus was repeatedly transiently suppressed using residual inhibition (RI) [1] following 30s masking stimuli (white noise). The subject provided feedback on tinnitus loudness at regular intervals (minimum 10 sec) for 3 blocks following each masker (Fig.1). For each trial spectral power was calculated in 10s epochs (sub-epoched into 1 s average) in 9 standard frequency bands (Fig.4f), following masker offset. For all analyses (oscillatory power, local cross-frequency coupling, within-frequency long-range coupling) Pearson product moment correlation coefficient was calculated between subjective tinnitus intensity and the measure of interest across trials for each frequency band for each electrode.

Conclusions

In a tinnitus patient with typical symptomatology, we provide the first clear demonstration of a distributed cortical 'tinnitus system', which incorporates a large proportion of the cerebral cortex, and all of the major oscillatory frequency bands. Tinnitus modulations were associated with complex restructuring of widespread within- and between-region neural coupling. The extent and cortical areas found to be involved with tinnitus change are in general agreement with recent proposals of a tinnitus network of brain regions [2].

References

1 Roberts LE. Residual inhibition. Prog Brain Res 166:487–95, 2007.

2 de Ridder D, Vanneste S, Weisz N, Londero A, Schlee W, Elgoyhen AB, Langguth B. An integrative model of auditory phantom perception: Tinnitus as a unified percept of interacting separable subnetworks. Neurosci Biobehav Rev 44:16–32, 2013.

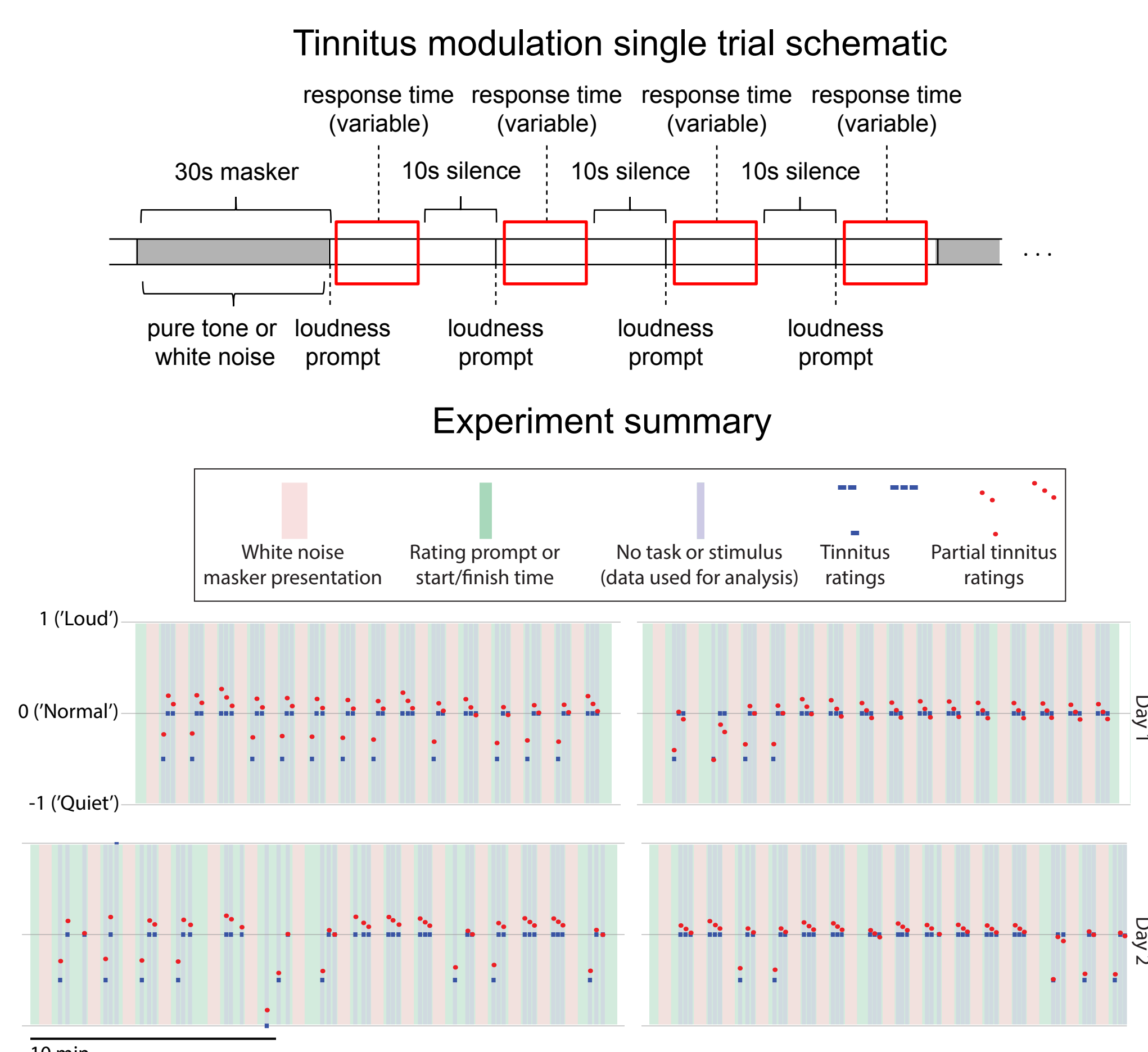
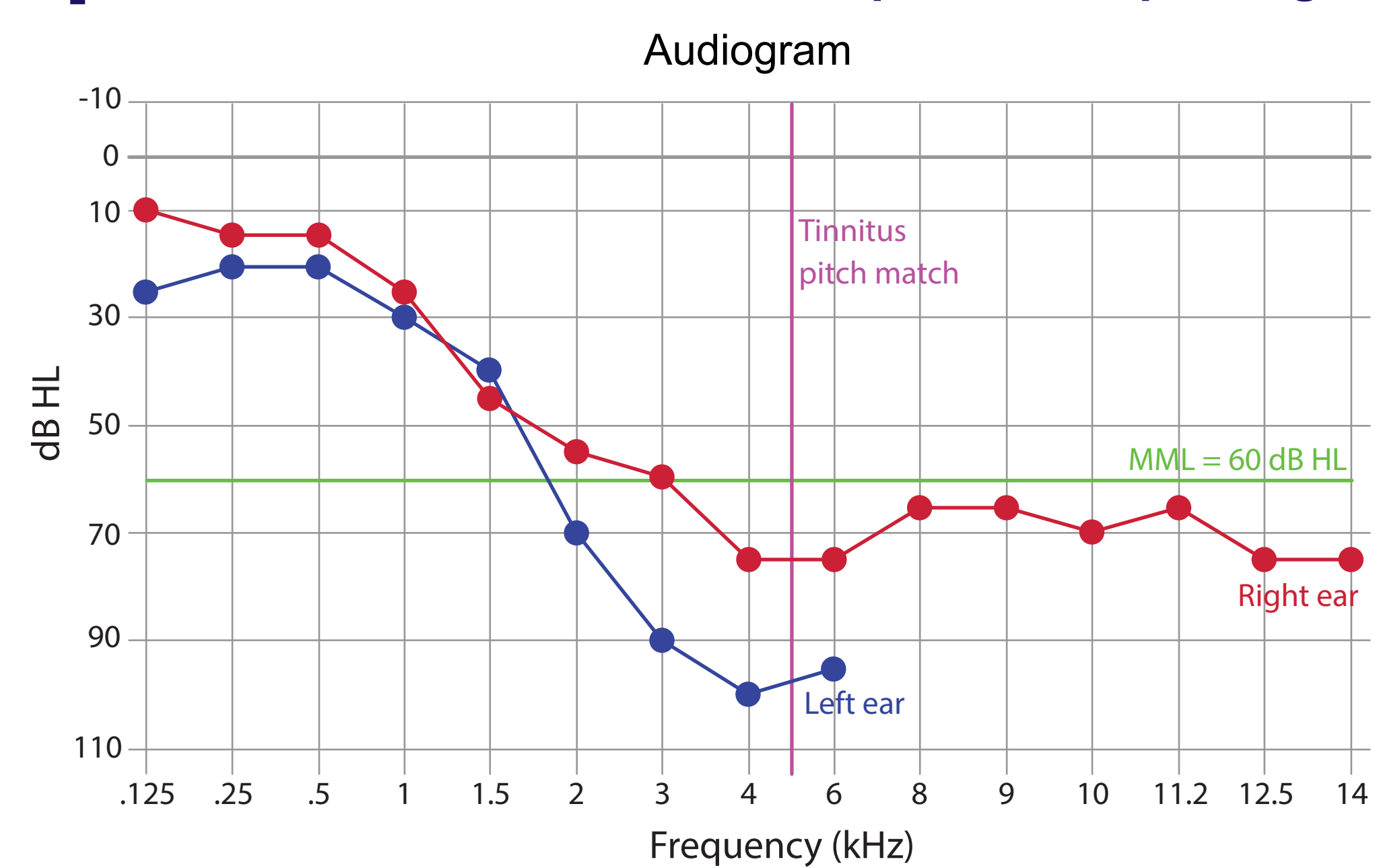
Acknowledgements

We thank Rich Tyler for clinical interview and Haiming Chen for help with data collection. This study was supported by Wellcome Trust Senior Clinical Fellowship WT091681, NIH R01-DC04290, R01-DC00657, UL1RR024979, and the Hoover Fund.

Contact information

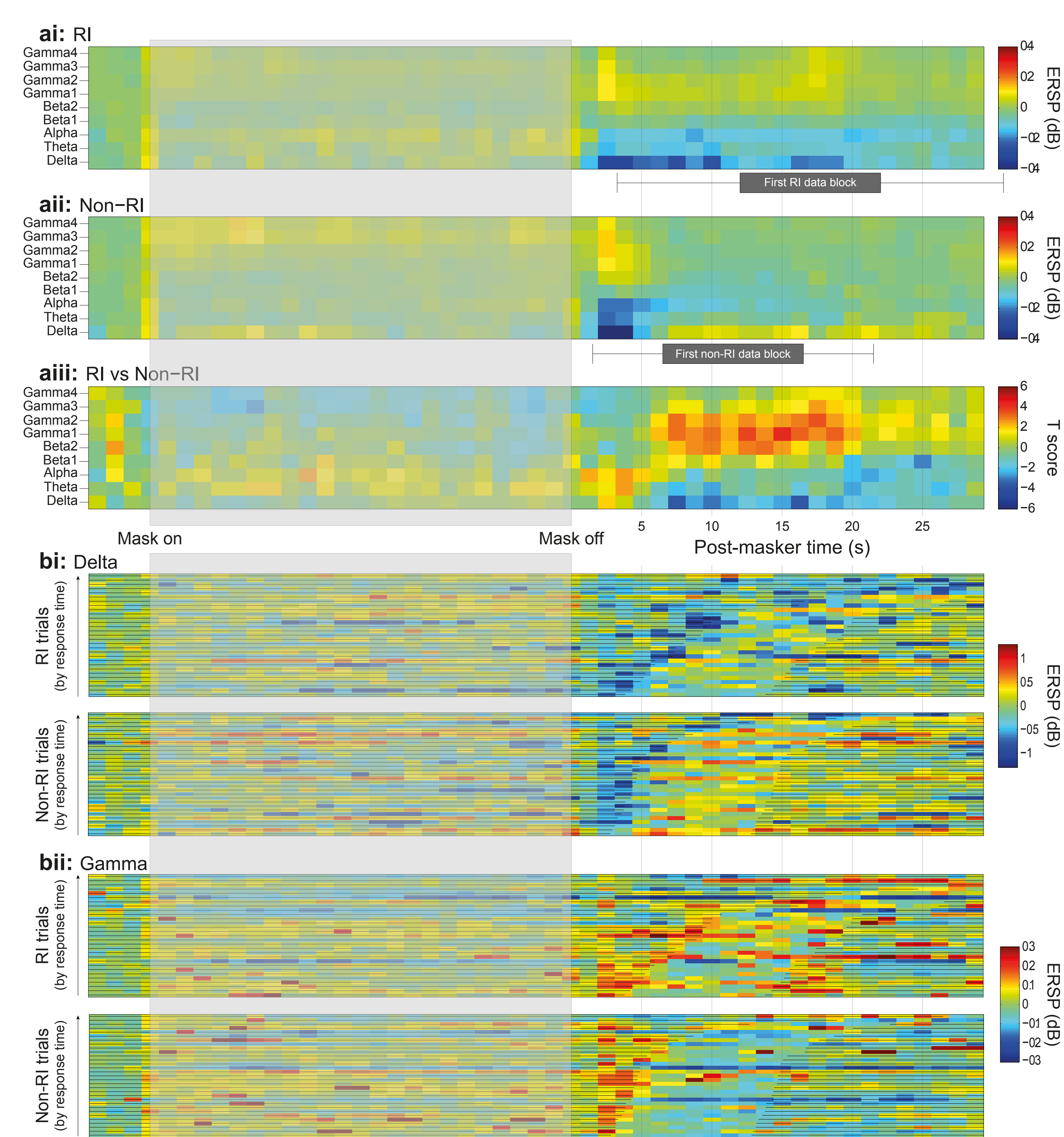
William Sedley, MD william.sedley@ncl.ac.uk
Phillip Gander, PhD phillip-gander@uiowa.edu

1 Tinnitus characteristics and experimental paradigm



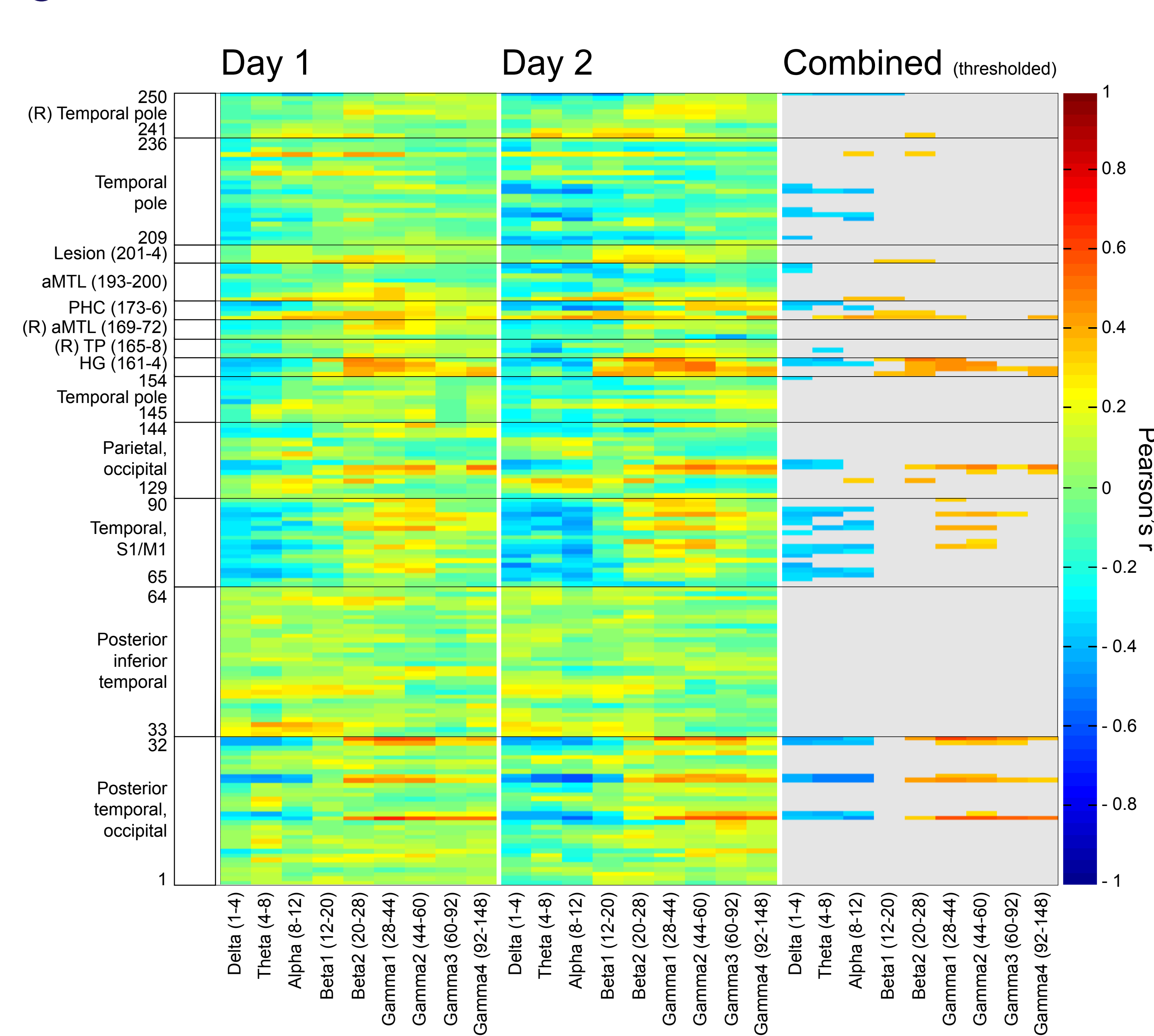
Approximately half of the trials resulted in tinnitus modulation, almost all of which were in the direction of suppression (residual inhibition). The behavioural results were nearly identical on two separate days (upper and lower rows). RI was induced by white noise.

2 Peri-masker power changes



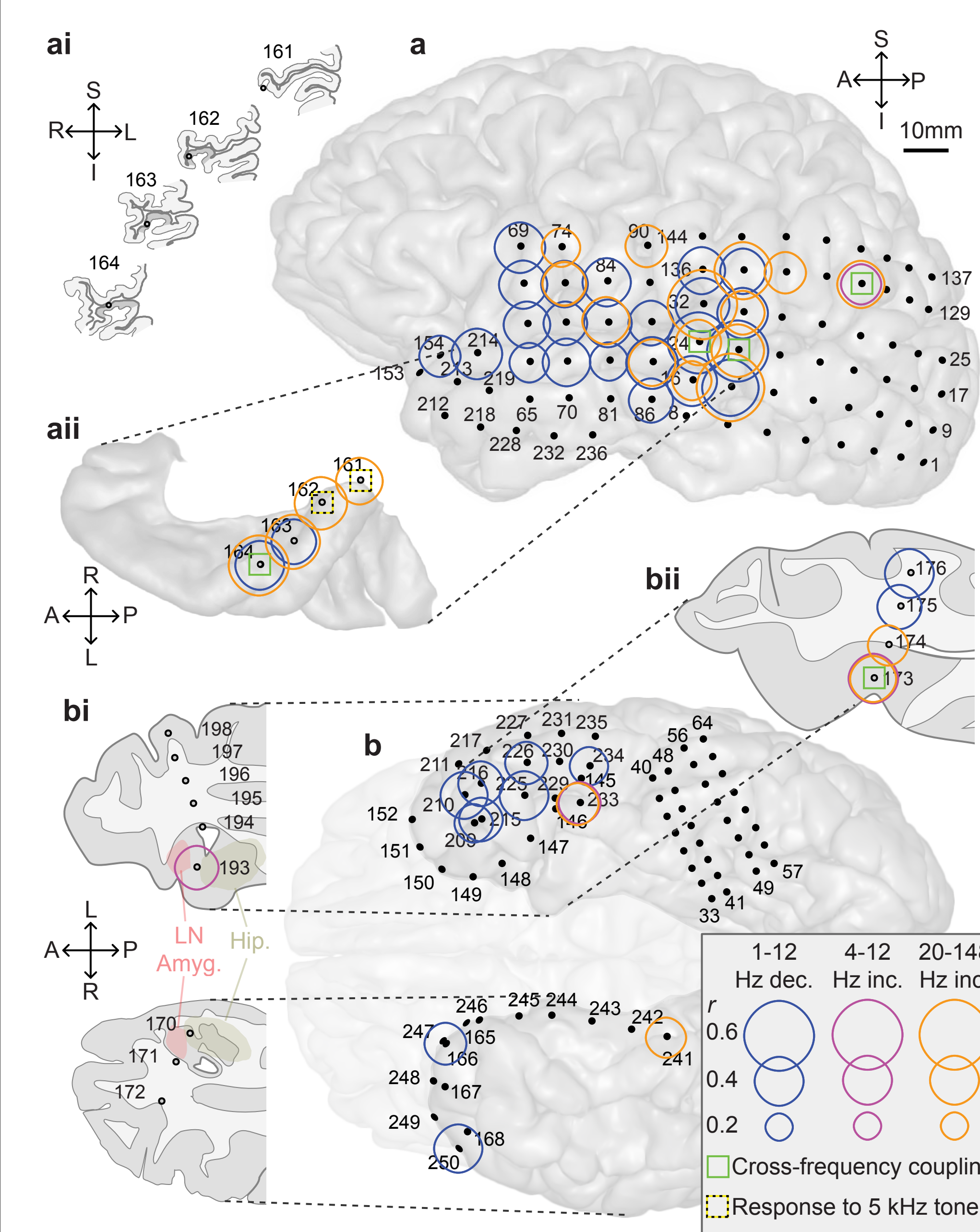
Time-frequency representations are shown for the time period before, during, and after the presentation of 30s noise maskers (gray shaded region) used to elicit residual inhibition. **a** Power changes are compared for trials which resulted in a suppression of tinnitus (RI) to those in which the tinnitus was unchanged (Non-RI). Frequency bands are described in Fig.6f. **i**) RI trials with mean and SD of the time period used for analysis following the loudness rating. **ii**) Non-RI trials with mean and SD of the time period used for analysis following the loudness rating. **iii**) T-score difference of Non-RI subtracted from RI trials. **b** Trial by trial power changes sorted according to the time taken to give a rating. Each row represents one trial; the horizontal lines indicate times when either the masker was playing or the subject was considering or providing a rating; time periods without a horizontal line were used for analysis. **i**) Delta band power. Upper panel shows data for RI trials, with Non-RI trials on the lower panel. **ii**) Gamma band power (20-148Hz). Upper panel shows data for RI trials, with Non-RI trials on the lower panel.

3 Power changes with tinnitus suppression across days



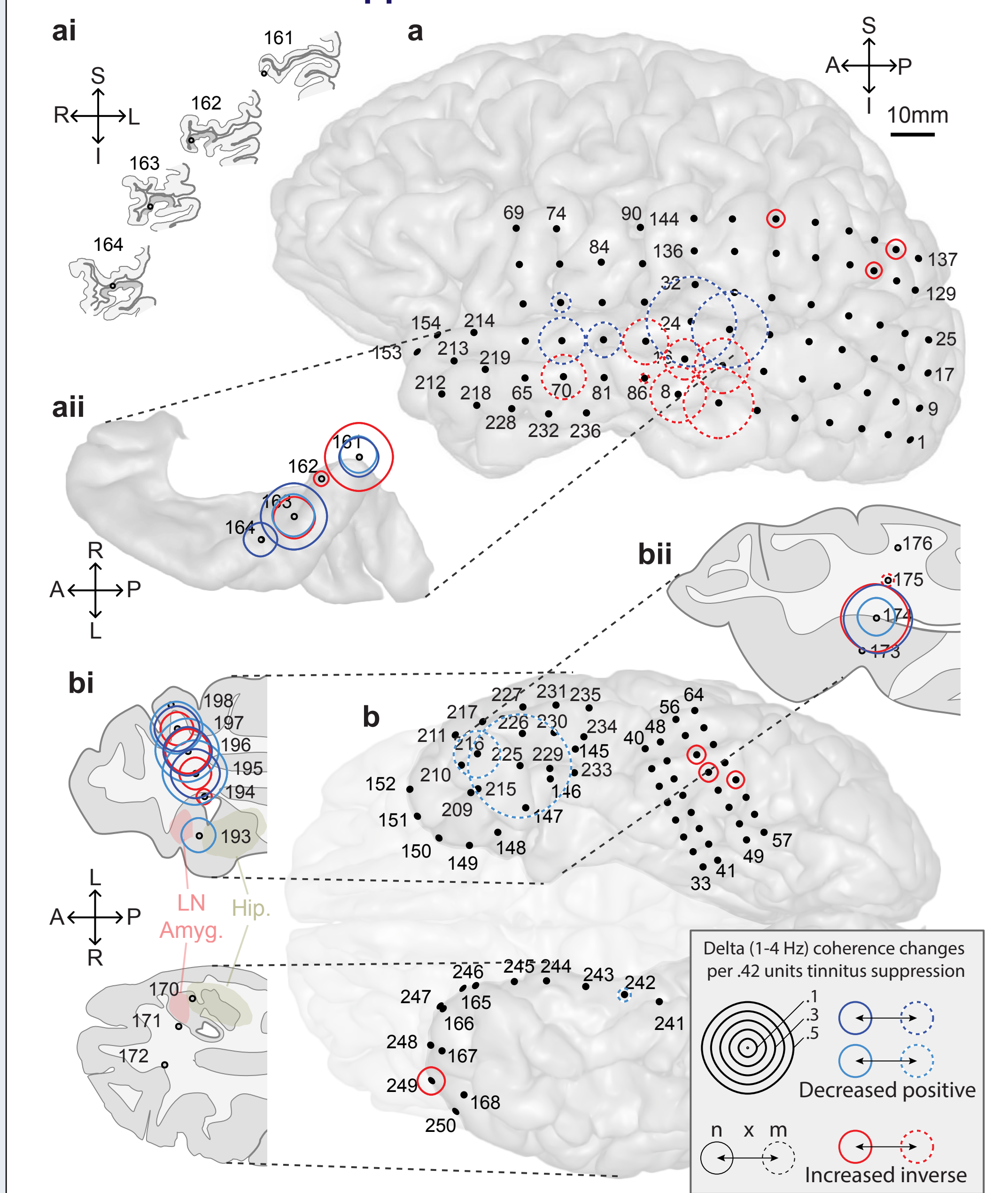
Oscillatory power changes correlating with tinnitus suppression are shown for two experimental sessions completed on subsequent days. Three data matrices are displayed, corresponding to (left to right) days 1 and 2 of the experiment, and the combined results thresholded at $p < 0.05$ corrected. Rows in the matrices represent individual electrodes (numbers correspond to those in Figure 4) and columns individual frequency bands (Hz). Color values denote the correlation coefficients (Pearson's r) between partial tinnitus suppression and power in any specific electrode/frequency combination. Cool colors indicate power decreases, with tinnitus suppression, and hot colors power increases. In the thresholded plot, gray colors indicate the absence of significant power change. S1/M1 = primary somatosensory/motor cortex, TP = temporal pole, HG = Heschl's gyrus, aMTL = anterior mesial temporal lobe, PHC = parahippocampal cortex.

4 Power changes with tinnitus suppression



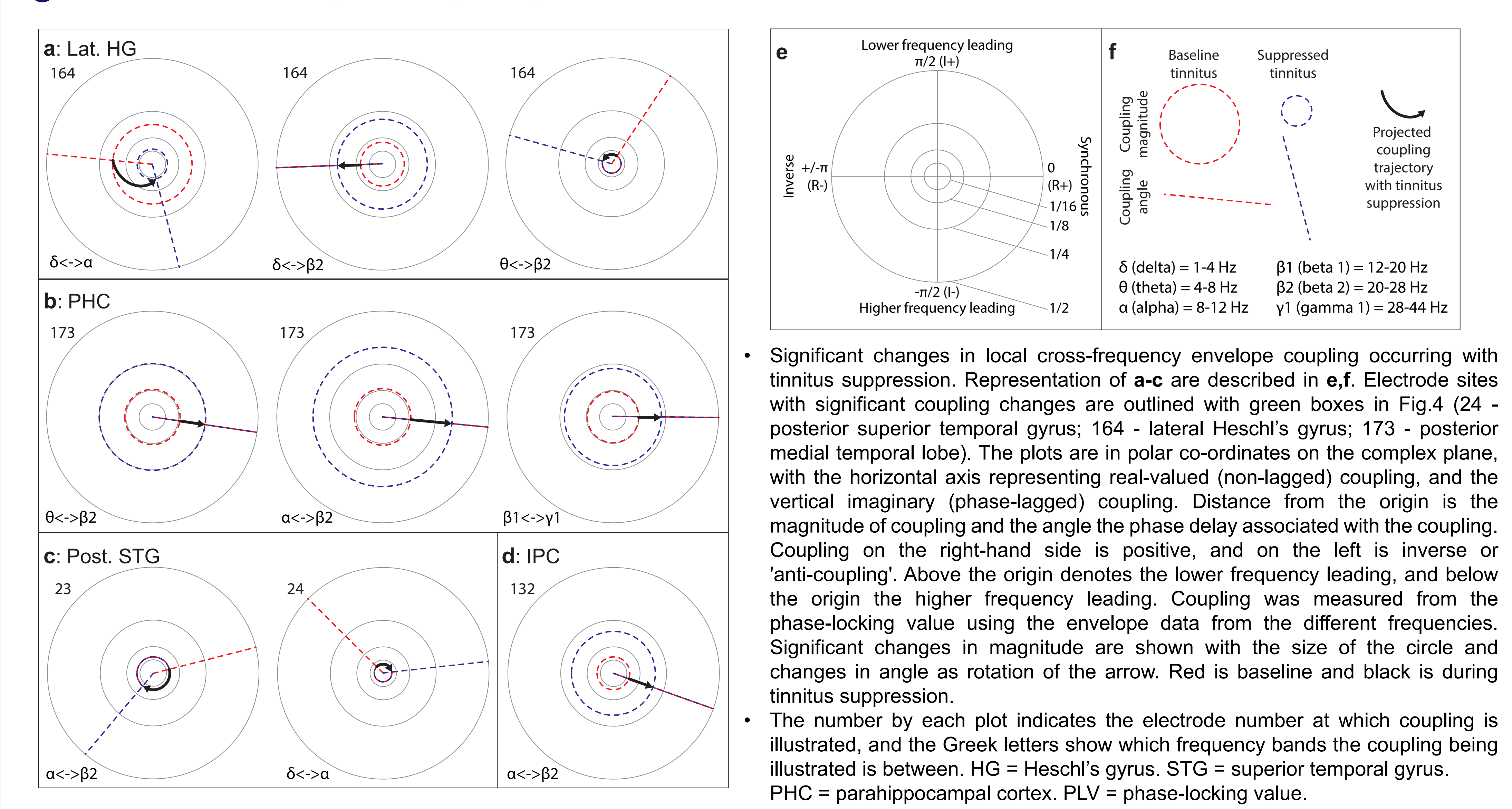
A pre-operative brain reconstruction is shown with electrode locations (black dots) estimated from the post-implantation CT and MRI scans. Circled electrodes denote significant power changes in a given frequency range following tinnitus suppression (see legend). **a** Left hemisphere. **i**) Coronal sections of Heschl's gyrus electrode locations. Heschl's gyrus is shaded dark grey. **ii**) Heschl's gyrus reconstruction with electrode locations. **b** Ventral view. **i**) Axial section line tracings showing electrode trajectory to left (top) and right (bottom) amygdala (coloured regions). **ii**) Axial section line tracing showing posterior hippocampal electrode trajectory.

5 Delta phase locking value changes with tinnitus suppression



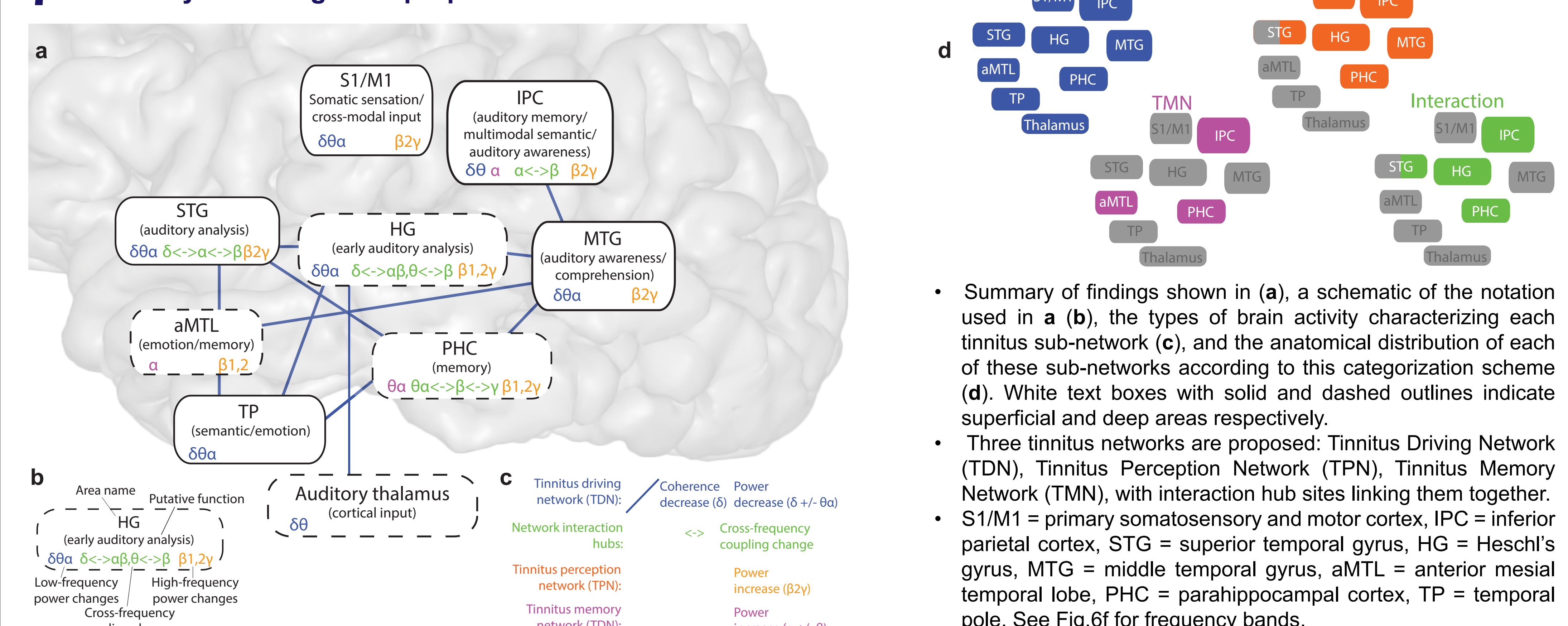
Delta-band (1-4Hz) inter-channel phase locking value (PLV) changes coinciding with tinnitus suppression. Significant PLVs were summarized using a principal component analysis with one positive (red) and two negative (blue, cyan) PCs. Direction of PLV change is shown in the legend. Each principal component indicates two separate sets of electrode weights (solid and dashed circles), the size of the circle denotes the magnitude of PLV change. **a** Left hemisphere. **i**) and **ii**) As describe in Fig.4. **b** Ventral view. **i**) and **ii**) As describe in Fig.4.

6 Local cross-frequency coupling changes with tinnitus suppression



Significant changes in local cross-frequency envelope coupling occurring with tinnitus suppression. Representation of **a-c** are described in **e,f**. Electrode sites with significant coupling changes are outlined with green boxes in Fig.4 (24 - posterior superior temporal gyrus; 164 - lateral Heschl's gyrus; 173 - posterior medial temporal lobe). The plots are in polar co-ordinates on the complex plane, with the horizontal axis representing real-valued (non-lagged) coupling, and the vertical imaginary (phase-lagged) coupling. Distance from the origin is the magnitude of coupling and the angle the phase delay associated with the coupling. Coupling on the right-hand side is positive, and on the left is inverse or 'anti-coupling'. Above the origin denotes the lower frequency leading, and below the origin the higher frequency leading. Coupling was measured from the phase-locking value using the envelope data from the different frequencies. Significant changes in magnitude are shown with the size of the circle and changes in angle as rotation of the arrow. Red is baseline and black is during tinnitus suppression.
• The number by each plot indicates the electrode number at which coupling is illustrated, and the Greek letters show which frequency bands the coupling being illustrated is between. HG = Heschl's gyrus. STG = superior temporal gyrus. PHC = parahippocampal cortex. PLV = phase-locking value.

7 Summary of findings and proposed tinnitus networks



Summary of findings shown in (a), a schematic of the notation used in (b), the types of brain activity characterizing each tinnitus sub-network (c), and the anatomical distribution of each of these sub-networks according to this categorization scheme (d). White text boxes with solid and dashed outlines indicate superficial and deep areas respectively.
• Three tinnitus networks are proposed: Tinnitus Driving Network (TDN), Tinnitus Perception Network (TPN), Tinnitus Memory Network (TMN), with interaction hub sites linking them together.
• S1/M1 = primary somatosensory and motor cortex, IPC = inferior parietal cortex, STG = superior temporal gyrus, HG = Heschl's gyrus, MTG = middle temporal gyrus, aMTL = anterior mesial temporal lobe, PHC = parahippocampal cortex, TP = temporal pole. See Fig.6f for frequency bands.